

# Spectrum Allocation and Power Control for Non-Orthogonal Multiple Access in HetNets

Jingjing Zhao, *Student member, IEEE*, Yuanwei Liu, *Member, IEEE*, Kok Keong Chai, *Member, IEEE*, Arumugam Nallanathan, *Fellow, IEEE*, Yue Chen, *Senior Member, IEEE*, and Zhu Han, *Fellow, IEEE*

**Abstract**—In this paper, a novel resource allocation design is investigated for non-orthogonal multiple access (NOMA) enhanced heterogeneous networks (HetNets), where small cell base stations (SBSs) are capable of communicating with multiple small cell users (SCUs) via the NOMA protocol. With the aim of maximizing the sum rate of SCUs while taking the fairness issue into consideration, a joint problem of spectrum allocation and power control is formulated. Particularly, the spectrum allocation problem is modeled as a many-to-one matching game with *peer effects*. We propose a novel algorithm where the SBSs and resource blocks (RBs) interact to decide their desired allocation. More importantly, we introduce the concept of ‘experimentation’ into the matching game for further improving the SCUs’ sum rate. The proposed algorithm is proved to converge to a two-sided exchange-stable matching. The power control of each SBS is formulated as a non-convex problem, where the sequential convex programming is adopted to iteratively update the power allocation result by solving the approximate convex problem. The obtained solution is proved to satisfy the Karush-Kuhn-Tucker (KKT) conditions. We unveil that: 1) The proposed algorithm closely approaches the optimal solution within a limited number of iterations; 2) The ‘experimentation’ action is capable of further enhancing the performance of the matching algorithm; and 3) The developed NOMA-enhanced HetNets achieve a higher SCUs’ sum rate compared to the conventional OMA-based HetNets.

**Index Terms**—Fairness, heterogeneous networks (HetNets), matching game, non-orthogonal multiple access (NOMA), sequential convex programming, sum rate.

## I. INTRODUCTION

To meet the surging traffic demands for wireless services and the need for high data rates, cellular networks are trending strongly towards heterogeneity of cells with different transmit power, coverage range and cost of deployment [1–3]. Heterogeneous networks (HetNets) is capable of achieving more spectrum-efficient communications by deploying small cells, i.e., picocells and femtocells, overlaid on the macrocells. Since the spectrum sharing among multi-tier cells causes both co-tier and cross-tier interference, efficient resource allocation and interference management become the fundamental research challenges for HetNets. In [4], a unified static framework was employed to study the interplay of user association and resource allocation in heterogeneous cellular networks. A novel solution that jointly associated the users to the access

points (APs), and allocated the femtocell access points (FAPs) to the service providers (SPs) in an uplink OFDMA network was studied in [5], with the aim of maximizing the total satisfaction of users. Considering the device-to-device (D2D)-enabled multi-tier scenario, a polynomial time-complexity distributed solution approach for the heterogeneous cellular mobile communication systems was presented in [6].

Recently, the non-orthogonal multiple access (NOMA) technique has attracted significant research interests for its potential to enhance spectrum efficiency by allowing multiple users simultaneous transmission in the same resource block (RB) [7]. More specifically, the fundamental concept of NOMA is to facilitate the access of multiple users in an extra dimension—power domain, via different power levels, which is different from conventional orthogonal multiple access (OMA) techniques. Regarding single carrier NOMA systems, considering users were randomly deployed in a disc, the performances of both outage probability and ergodic rate were investigated in [8]. The fairness issue of NOMA was investigated in [9] for a multiple-user scenario under two different CSI assumptions. In [10], under the assumption of only statistical channel state information (CSI) known at the transmitter, the power allocation and decoding order selection problem were investigated for achieving optimal outage performance. In [11], the problem of optimal power allocation when the transmitter only had the average CSI was studied in downlink NOMA systems. On the standpoint of energy aspects, a new cooperative NOMA transmission protocol was proposed in [12], in which near NOMA users were regarded as energy harvesting user relays for forwarding messages to far NOMA users.

It is worth noting that besides power domain multiplexing gain brought by NOMA, multi-carrier systems are capable of providing additional degrees of freedom offered by multiuser diversity, which motivates researchers to work on multi-carrier NOMA systems. Some initial research contributions in terms of resource allocation have been done for NOMA multi-carrier/cluster/subchannel scenarios [13–17]. In [13], the authors jointly investigated the power and subcarrier allocation problem in multi-carrier NOMA systems, where the BS worked in a full-duplex mode. Both the optimal performance with applying a monotonic optimization approach and the sub-optimal performance with applying a low complexity iterative approach were demonstrated. In [14], the subchannel assignment and power allocation are jointly optimized to maximize the weighted total sum-rate in the NOMA system, while taking into account of the users’ fairness. For maximizing the energy efficiency of the downlink multi-carrier NOMA systems, a

J. Zhao, K. K. Chai, and Y. Chen are with Queen Mary University of London, London, United Kingdom (email: {j.zhao, michael.chai, yue.chen}@qmul.ac.uk).

Y. Liu and A. Nallanathan are with King’s College London, London, United Kingdom (email: {yuanwei.liu, arumugam.nallanathan}@kcl.ac.uk).

Z. Han is with University of Houston, Houston, Tx, USA (email: zhan2@uh.edu).

low complexity suboptimal subchannel assignment and power proportional factors determination algorithm was proposed in [15], by assuming two users were assigned in the same channel. In [16], under the assumption of knowing statistical CSI at the BS, a power-efficient resource allocation scheme was studied for MC-NOMA systems. Moreover, the proposed design in [16] also investigated the successive interference cancelation (SIC) decoding order according to different level of quality of service (QoS). For multiple-input and multiple-output (MIMO) NOMA scenarios, the performance was studied in [17] based on a clustered based MIMO-NOMA structure on the standpoint of investigating the fairness issue.

### A. Motivation and Contributions

Despite the fact that there are ongoing research efforts to address the resource allocation problems for both HetNets and NOMA, to the best of our knowledge, the solutions for the resource allocation problems in NOMA-enhanced HetNets have not been studied in the literature. Note that NOMA-enhanced HetNets design poses additional challenges in terms of interference management since it brings additional co-channel interference to the existing networks. As such, novel resource allocation design for intelligently managing and coordinating various types of interference are more than desired, which motivates us to develop this treatise. We focus on studying the joint spectrum and power allocation problem for NOMA-enhanced HetNets with the aim of maximizing the sum rate of small cell users (SCUs). Particularly, we consider the downlink scenario, where one macro base station (MBS) communicates with multiple macro cell users (MCUs) via the conventional OMA protocol, and each small base station (SBS) communicates with two NOMA SCUs.

To tackle the formulated problem, we decouple the spectrum and power allocation problems and provide a joint solution where the spectrum and power allocation are executed iteratively. For the spectrum allocation, we allow multiple SBSs to reuse the same RB occupied by a MCU to improve the resource utilization. We recognize that the spectrum allocation can be regarded as a many-to-one matching process between the SBSs and RBs, where the SBSs and RBs act as two sets of players and interact with each other to maximize the sum rate of SCUs. In addition, the SBSs have *peer effects* with the interdependencies among each other due to the co-channel interference. Therefore, to solve this problem, we adopt the matching theory [18, 19], which provides mathematically tractable and low-complexity solutions for the combinatorial problem of matching players in two distinct sets [20]. We then formulate the spectrum allocation problem as a many-to-one matching problem with *peer effects* and propose efficient algorithms to solve the problem. The primary contributions of this paper can be summarized as follows.

- 1) We propose a new NOMA-enhanced HetNets model, in which NOMA technique is invoked in small cells for spectrum efficiency enhancement and user access improvement. Based on the proposed model, we formulate a joint spectrum allocation and power control problem with the aim of maximizing SCUs' sum rate while considering users' fairness issues.

- 2) We model the spectrum allocation for SBSs as a many-to-one matching problem with *peer effects*. For solving the formulated problem, we first propose a swap-operation enabled matching algorithms (SOEMA-1) to match SBSs with RBs aiming at maximizing SCUs' sum rate. For further improving the performance of SOEMA-1, we introduce the concept of 'experimentation' into the matching game and propose a novel algorithm SOEMA-2, where irrational swap decisions are enabled with a small probability to explore the potential matching states.
- 3) To solve the non-convex power control problem of each SBS, we invoke the sequential convex programming to iteratively update the power allocation vector by solving the approximate convex problem. We prove that the proposed algorithm is convergent and the solution satisfies the Karush-Kuhn-Tucker (KKT) conditions.
- 4) We demonstrate that NOMA-enhanced HetNets is capable of significantly outperforming the conventional OMA based HetNets in terms of both the SCUs' sum rate and users' connectivity. Additionally, we also present that the performance of the matching algorithm can be further improved via the 'experimentation' action.

### B. Organization and Notations

The rest of this paper is organized as follows. In Section II, the system model of NOMA-enhanced HetNets is studied. Section III introduces the SCUs' fairness achieved by the  $\alpha$ -utility function and formulates the optimization problem. Section IV and Section V solve the spectrum allocation and power control problems, respectively. Numerical results are presented in Section VI, followed by the conclusions in Section VII. The notation of this paper is shown in Table I.

TABLE I: Notation

$SBS, SCU$	Set of SBSs and SCUs
$MCU, RB$	Set of MCUs and RBs
$B, M, K$	Number of SBSs, RBs, and SCUs served by each SBS
$\lambda$	Spectrum sharing indicator
$\mathbf{a}$	Power allocation coefficient
$f, h, g$	Channel coefficients
$p_b$	Total transmit power of SBSs
$p_m$	Transmit power of MBS on each MCU
$\zeta$	Additive white Gaussian noise with variance $\sigma^2$
$I_{co}, I_{cr}$	Co-tier and cross-tier interference
$I_N$	Interference of superposition signals via NOMA

## II. NETWORK MODEL

### A. System Description

Consider a downlink  $K$ -tier HetNets model, where the first tier represents a single macro cell and the other tiers represent the small cells such as pico cells and femto cells. The MBS provides the basic coverage, and SBSs are deployed in the coverage area of the MBS to enhance capability. The set of SBSs is represented by  $SBS = \{1, \dots, B\}$ . The MBS serves a set of  $M$  MCUs, i.e.,  $MCU = \{1, \dots, M\}$ . There are  $M$  RBs, and each MCU occupies a RB. For the sake of simplicity, we use the same index of the RBs as the MCUs, and thus the set

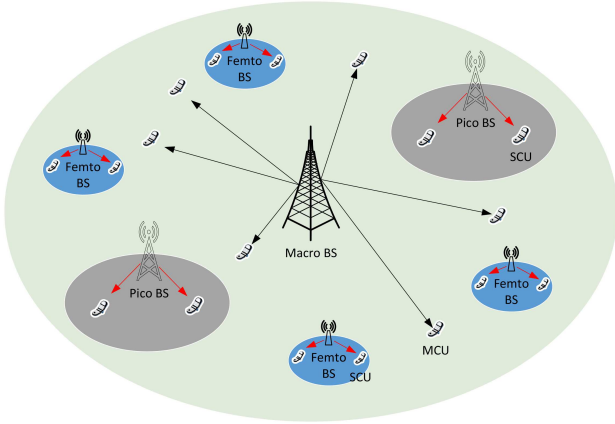


Fig. 1: Illustration of NOMA-enhanced HetNets.

of RBs is represented by  $\mathcal{RB} = \{1, \dots, M\}$ . The macro cell and small cells reuse the same set of RBs, and thus we refer to the small cells as the underlay tier. In this paper, we assume that each SBS  $b$  occupies no more than one RB and serves at most two SCUs simultaneously via the NOMA protocol. This assumption is attributed to limit the co-channel interference and to lower the hardware complexity and processing delay<sup>1</sup>. The illustration of cellular layout is shown in Fig. 1.

In this work, we allow multiple SBSs to reuse the same RB to improve the spectrum efficiency. The maximum number of SBSs occupying the same RB is restricted to  $q_{max}$ . We assume that the total number of SBSs allowed for spectrum access, i.e.,  $M \times q_{max}$ , is larger than  $B$ . Thus, all the SBSs can be served. Since the spectrum sharing brings in both co-tier and cross-tier interference, efficient resource allocation is required for the NOMA-enhanced HetNets system. In our work, we assume that the user association to the MBS and SBSs are completed prior to the resource allocation.

## B. Channel Model

The NOMA based transmission requires to apply the superposition coding (SC) technique at the SBSs and SIC<sup>2</sup> technique at the SCUs. The vector  $\mathbf{a}_b = [a_{b,k}, a_{b,j}]$  represents the power allocation coefficients for the SCUs in each small cell. The SBS  $b$  sends messages to SCUs  $k$  and  $j$  on RB  $m$ , based on the NOMA principle, i.e.,  $b$  sends  $a_{b,k}x_{b,k}^m + a_{b,j}x_{b,j}^m$ , where  $x_{b,k}^m$  is the message for SCU  $k$ . The received signal at SCU  $k$  served by the  $b$ -th SBS, i.e.,  $b \in \{1, \dots, B\}$ , on the  $m$ -th RB

<sup>1</sup>NOMA requires SIC at the receivers. A user performing SIC needs to demodulate and decode the signals transmitted to other receivers. Therefore, the hardware complexity and processing delay increases with the number of users multiplexed on the same RB.

<sup>2</sup>It is assumed that perfect SIC is achieved at the receivers. In practical scenarios, proceeding perfect SIC may be a non-trivial task. Therefore, our work actually provides an upper bound in terms of the attainable data rates.

is given by

$$y_{b,k}^n = \underbrace{f_{b,k}^m \sqrt{p_b a_{b,k}} x_{b,k}^m}_{\text{desired signal}} + \underbrace{f_{b,k}^m \sqrt{p_b a_{b,j}} x_{b,j}^m}_{\text{interference from NOMA users}} + \underbrace{\zeta_{b,k}^m}_{\text{noise}} + \underbrace{\sum_{m=1}^M \lambda_{m,b} h_{m,b,k} \sqrt{p_m} x_m}_{\text{cross-tier interference}} + \underbrace{\sum_{b^* \neq b} \lambda_{b^*,b} g_{b^*,b,k}^m \sqrt{p_{b^*}} x_{b^*}^m}_{\text{co-tier interference}}, \quad (1)$$

where  $x_{b,k}^m$ ,  $x_m$  are the symbols transmitted from the  $b$ -th SBS to its serving SCU  $k$ , i.e.,  $SCU_{b,k}$ , and from the MBS to the MCU  $m$ , respectively.  $f_{b,k}^m$ ,  $h_{m,b,k}$ , and  $g_{b^*,b,k}^m$  are the channel coefficients between SBS  $b$  and  $SCU_{b,k}$ , that between the MBS and  $SCU_{b,k}$ , and that between SBS  $b^*$  and  $SCU_{b,k}$  on RB  $m$ , respectively.  $p_b$  and  $p_m$  are the total transmit power of the SBS  $b$  and the transmit power from the MBS to the MCU  $m$ , respectively.  $\lambda_{m,b}$  represents the RB allocation indicator for SBSs, i.e., if SBS  $b$  occupies RB  $m$ ,  $\lambda_{m,b} = 1$ ; otherwise,  $\lambda_{m,b} = 0$ .  $\lambda_{b^*,b}$  represents the presence of co-tier interference, i.e., if the SBS  $b$  and  $b^*$  reuse the same RB,  $\lambda_{b^*,b} = 1$ ; otherwise,  $\lambda_{b^*,b} = 0$ .  $\zeta_{b,k}^m$  is the additive white gaussian noise (AWGN) at  $SCU_{b,k}$  with variance  $\sigma^2$ .

NOMA systems exploit the power domain for multiple access, where different users are served at different power levels. For illustration, assume SCU  $j$  desires to decode and remove interference from the superposition signal of SCU  $k$  via SIC. The interference cancellation is successful if the SCU  $j$ 's received SINR for the SCU  $k$ 's signal is larger or equal to the received SINR of SCU  $k$  for its own signal [8, 13]. Therefore, the condition of our given SIC decoding order is given by

$$\frac{|f_{b,j}^m|^2 p_b a_{b,k}^m}{I_N^{j,k} + I_{co}^j + I_{cr}^j + \sigma^2} \geq \frac{|f_{b,k}^m|^2 p_b a_{b,k}^m}{I_N^{k,k} + I_{co}^k + I_{cr}^k + \sigma^2}. \quad (2)$$

The inequality in (2) can be rewritten in the following:

$$|f_{b,j}^m|^2 (I_{co}^k + I_{cr}^k + \sigma^2) - |f_{b,k}^m|^2 (I_{co}^j + I_{cr}^j + \sigma^2) \geq 0. \quad (3)$$

Therefore, according to the received signal expressed in (1), the received SINR at SCU  $k$  served by the  $b$ -th SBS on RB  $m$  to decode its own information is given by

$$\gamma_{b,k,k}^m = \frac{|f_{b,k}^m|^2 p_b a_{b,k}^m}{I_N^{k,k} + I_{co}^k + I_{cr}^k + \sigma^2}, \quad (4)$$

where  $I_N^{k,k} = |f_{b,k}^m|^2 p_b a_{b,j}^m$  is the interference from the superposed signal to SCU  $j$ ,  $I_{co}^k = \sum_{b^* \neq b} \lambda_{b^*,b} p_{b^*} |g_{b^*,b,k}^m|^2$  is the co-tier interference from the other SBSs reusing the same RB, and  $I_{cr}^k = \sum_m \lambda_{m,b} p_m |h_{m,b,k}|^2$  is the cross-tier interference from the MBS. Here,  $|f_{b,k}^m|^2 = |\hat{f}_{b,k}^m|^2 (d_{b,k})^{-\alpha}$ ,  $|g_{b^*,b,k}^m|^2 = |\hat{g}_{b^*,b,k}^m|^2 (d_{b^*,b,k})^{-\alpha}$ , and  $|h_{m,b,k}|^2 = |\hat{h}_{m,b,k}|^2 (d_{m,b,k})^{-\alpha}$ .  $\hat{f}_{b,k}^m$ ,  $\hat{g}_{b^*,b,k}^m$  and  $\hat{h}_{m,b,k}$  are small-scale fading with  $\hat{f}_{b,k}^m \sim \mathcal{CN}(0, 1)$ ,  $\hat{g}_{b^*,b,k}^m \sim \mathcal{CN}(0, 1)$  and  $\hat{h}_{m,b,k} \sim \mathcal{CN}(0, 1)$ .  $d_{b,k}$  is the distance from SBS  $b$  to  $SCU_{b,k}$ .  $d_{b^*,b,k}$  is the distance

from SBS  $b^*$  to  $SCU_{b,k}$ , and  $d_{m,b,k}$  is the distance from the MBS to  $SCU_{b,k}$ .

Note that SCU  $j$  can decode the signal to SCU  $k$ , thus the SINR received at SCU  $j$  is expressed as

$$\gamma_{b,j}^m = \frac{|f_{b,j}^m|^2 p_b a_{b,j}^m}{I_{co}^j + I_{cr}^j + \sigma^2}. \quad (5)$$

To guarantee the service qualities of the MCUs, we give an interference threshold  $I_{thr}$  to the aggregated interference caused to the MCUs from the links in the underlay tier. The aggregated interference experienced on the MCU  $m$  is given by

$$I_m = \sum_{b=1}^B \lambda_{m,b} p_b |t_{b,m}|^2, \quad (6)$$

where  $|t_{b,m}|^2 = |\hat{t}_{b,m}|^2 (d_{b,m})^{-\alpha}$ , and  $\hat{t}_{b,m}$  is small-scale fading with  $\hat{t}_{b,m} \sim \mathcal{CN}(0, 1)$ .  $d_{b,m}$  is the distance from SBS  $b$  to MCU  $m$ .

### III. PROBLEM FORMULATION

In this section, we first define the  $\alpha$ -utility function for SCUs' data rates to guarantee the fairness among the SCUs served by each SBS. Then we formulate the SCUs' sum rate maximization problem via proper spectrum and power allocation.

#### A. SCUs' Fairness Based on $\alpha$ -Utility Function

Based on the SINR expressions of SCU  $k$  and  $j$  in (4) and (5), the data rates of SCU  $k$  and  $j$  served by SBS  $b$  over RB  $m$  can be calculated as

$$R_{b,k}^m = \lambda_{m,b} \log_2 \left( 1 + \frac{|f_{b,k}^m|^2 p_b a_{b,k}^m}{I_N^{k,k} + I_{co}^k + I_{cr}^k + \sigma^2} \right), \quad (7)$$

and

$$R_{b,j}^m = \lambda_{m,b} \log_2 \left( 1 + \frac{|f_{b,j}^m|^2 p_b a_{b,j}^m}{I_{co}^j + I_{cr}^j + \sigma^2} \right), \quad (8)$$

respectively. For the SCUs served by the same SBS, the optimal power allocation is to allocate the total transmit power to the SCU with the best channel condition [21]. To guarantee the rate fairness among the SCUs served by the same SBS, we adopt the  $\alpha$ -proportional fairness, where the  $\alpha$ -utility function of SCU  $k$  served by SBS  $b$  is defined as [22]

$$U_\alpha(R_{b,k}^m) = \begin{cases} \ln R_{b,k}^m, & \text{if } \alpha = 1 \\ (1 - \alpha)^{-1} (R_{b,k}^m)^{1-\alpha}, & \text{if } 0 \leq \alpha < 1. \end{cases} \quad (9)$$

Based on the defined  $\alpha$ -utility function, the  $\alpha$ -fairness based sum rate of SBS  $b$  is expressed as:

$$U_\alpha(R_b^m(\lambda, \mathbf{a})) = U_\alpha(R_{b,k}^m) + U_\alpha(R_{b,j}^m). \quad (10)$$

#### B. Optimization Problem Formulation

For facilitating the presentation, we denote  $\lambda \in \mathbb{R}^{M \times B}$ ,  $\mathbf{a} \in \mathbb{R}^{B \times 2}$  as the collections of optimization variables  $\lambda_{m,b}$ , and  $a_{b,k}$ , respectively. The system objective is to maximize the sum  $\alpha$  utility of the SCUs with interference constraints for the MCUs satisfied, which can be expressed as follows:

$$\max_{\lambda, \mathbf{a}} \sum_{b=1}^B \sum_{m=1}^M U_\alpha(R_b^m(\lambda, \mathbf{a})), \quad (11a)$$

$$s.t. \quad \sum_{b=1}^B \lambda_{m,b} p_b |t_{b,m}|^2 \leq I_m^{thr} \quad \forall m, \quad (11b)$$

$$|f_{b,j}^m|^2 (I_{co}^k + I_{cr}^k + \sigma^2) - |f_{b,k}^m|^2 (I_{co}^j + I_{cr}^j + \sigma^2) \geq 0, \quad (11c)$$

$$\lambda_{m,b} \in \{0, 1\}, \quad \forall m, b, \quad (11d)$$

$$\sum_m \lambda_{m,b} \leq 1, \quad \forall b, \quad (11e)$$

$$\sum_b \lambda_{m,b} \leq q_{max}, \quad \forall m, \quad (11f)$$

$$a_{b,k} \geq 0, a_{b,j} \geq 0, \quad \forall b, \quad (11g)$$

$$a_{b,k} + a_{b,j} \leq 1, \quad \forall b. \quad (11h)$$

With the constraint in (11b), the aggregated interference caused to the MCU  $m$  by the underlay transmitters reusing the same RB is restricted by a predefined threshold, i.e.,  $I_m^{thr}$ . Constraint (11c) guarantees successful SIC at SCU  $j$ . Constraints (11d) and (11e) are imposed to guarantee that each SBS occupies no more than one RB. Constraint (11f) limits the maximum number of SBSs, i.e.,  $q_{max}$ , reusing each RB. Constraint (11g) is the non-negative transmit power constraint for the SBSs. Constraint (11h) gives the upper bound of the transmit power of the SBSs.

The formulated problem is a mixed combinatorial non-convex problem due to the binary constraint for RB allocation in (11d) as well as the non-convex objective function. In general, there is no systematic and computational efficient approach to solve this problem optimally. As can be observed, the optimization problem in (11) is coupled by the two problems of spectrum allocation and power control. To reduce the computational complexity, we decouple these two subproblems as the following. For any fixed power allocation, the spectrum allocation for SBSs is formulated as a many-to-one matching game [19] where the RBs and SBSs interact with each other to find the optimal matching. For the given spectrum allocation result, the power allocation problem for the SCUs is solved by applying the sequential convex programming [23]. We then propose a joint algorithm where the spectrum allocation and power control are performed iteratively to find the joint resource allocation result.

#### IV. MANY-TO-ONE MATCHING FOR SPECTRUM ALLOCATION

In this section, we first consider the spectrum allocation problem for SBSs given fixed power allocation. More particularly, for any given feasible power allocation, the original problem in (11) can be decomposed into the RB allocation problem for all the SBSs, which can be expressed as

$$\max_{\lambda} \sum_{b=1}^B \sum_{m=1}^M U_{\alpha}(R_b^m(\lambda)), \quad (12a)$$

$$s.t. \quad (11b) - (11f). \quad (12b)$$

For obtaining the global optimal solution of (12), we need to fully search all the possible combinations of scheduling RBs to SBSs. Thus, even for a centralized algorithm, it is not feasible in practical systems to solve it. However, since  $\lambda$  is a binary variable, we formulate the RB allocation as a many-to-one matching problem [19].

##### A. Many-to-One Matching Problem Formulation

To proceed with formulating the matching problem, we first introduce some important definitions..

**Definition 1.** *In the many-to-one matching model, a matching  $\Phi$  is a function from the set  $\mathcal{RB} \cup \mathcal{SBS}$  into the set of all subsets of  $\mathcal{RB} \cup \mathcal{SBS}$  such that 1)  $|\Phi(b)| = 1, \forall b \in \mathcal{SBS}$ ; 2)  $|\Phi(m)| \leq q_{max}, \forall m \in \mathcal{RB}$ ; 3)  $\Phi(b) = m$  if and only if  $b \in \Phi(m)$ .*

For the conditions in the definition, condition 1) implies that each SBS can only be matched with one RB; condition 2) gives the quota  $q_{max}$  of the maximum number of SBSs that can be matched to each RB; and condition 3) implies that if SBS  $b$  is matched with RB  $m$ , then RB  $m$  is also matched with SBS  $b$ .

The utility of SBS  $b$  is defined as the sum rate of all the serving SCUs minus its cost for occupying RB  $m$ , which is given by

$$U_b = \sum_{k=1}^K U_{\alpha}(R_{b,k}^m) - \beta p_b |g_{b,m}|^2, \quad (13)$$

where  $\beta \in \mathbb{R}^+$  is the fixed coefficient with unit interference of SBS  $b$  bringing to the  $m$ -th MCU.

The utility of RB  $m$  is defined as the sum rate of the occupying SCUs plus the fees it charges the SBSs for causing interference to the corresponding MCU, and thus the utility function of RB  $m$  can be expressed as

$$U_m = \sum_{b=1}^B \lambda_{m,b} \sum_{k=1}^K U_{\alpha}(R_{b,k}^m), \quad (14)$$

To start the matching process, both SBSs and RBs need to set up the preference lists with respect to their own interests. The preference list is a descending order list formed by each side of the players according to their preference to the other side of the players. For each SBS  $b$ , it forms a descending order preference list  $\mathcal{BLIST}_b$  according to its utilities over all the RBs. For example, if SBS  $b$  can achieve higher data rate

over RB  $m$  compared to RB  $m'$ , i.e.,  $U_b(m) > U_b(m')$ , we have  $m \succ_b m'$ , which indicates that  $b$  prefers  $m$  to  $m'$ . Since each RB can be matched with up to  $q_{max}$  SBSs, each RB  $m$  forms a preference list  $\mathcal{RBLIST}_m$  over all the possible sets of SBSs with the descending order of its utility. That is,  $U_m(\mathcal{S}) > U_m(\mathcal{S}') \Rightarrow \mathcal{S} \succ_m \mathcal{S}'$ , which refers that RB  $m$  prefers the set of SBS  $\mathcal{S}$  to  $\mathcal{S}'$ .

**Remark 1.** *The matching game formulated above is a many-to-one matching with peer effects.*

*Proof.* As observed in (4), (5) and (13), the utility of each SBS is affected by the co-tier interference from the SBSs occupying the same RB. In other words, the utility of each SBS depends not only on the RB it matches with, but also on which other SBSs match to the same RB. Therefore, the formulated game model is a many-to-one matching with *peer effects*.  $\square$

Due to the existence of peer effects in this matching model, the preference lists of players change with the matching game proceeds, which is different from conventional matching games where players have fixed preference lists [24, 25]. There is a growing literature studying many-to-one matchings with peer effects [26, 27]. However, these research contributions have demonstrated that designing matching mechanisms is significantly more challenging when peer effects are considered. Motivated by the housing assignment problem in [28], we propose an extended matching algorithm for the many-to-one matching problem with peer effects in the following.

**Remark 2.** *The formulated matching game is lack of the property of substitutability.*

*Proof.* See Appendix A.  $\square$

Due to the lack of substitutability, the traditional Gale Shapley (GS) Algorithm [18] do not apply to the formulated matching game any more. To better handle the interdependencies between the players' preferences, the *swap operations* between any two SBSs to exchange their matched RBs is enabled. We first define the concept of *swap matching* as follows:

$$\Phi_b^{b'} = \{\Phi \setminus \{(b, \Phi(b)), (b', \Phi(b'))\}\} \cup \{(b, \Phi(b')), (b', \Phi(b))\}, \quad (15)$$

where SBSs  $b$  and  $b'$  switch places while keeping other SBSs and RBs' matchings unchanged.

Based on the concept of *swap operations*, the *swap-blocking* pair is defined as follows:

**Definition 2.** *A pair of SBSs  $(b, b')$  is a swap-blocking pair if and only if*

- 1)  $\forall s \in \{b, b', \Phi(b), \Phi(b')\}, U_s(\Phi_b^{b'}) \geq U_s(\Phi)$  and;
- 2)  $\exists s \in \{b, b', \Phi(b), \Phi(b')\}$ , such that  $U_s(\Phi_b^{b'}) > U_s(\Phi)$ , where  $U_s(\Phi)$  represents the utility of the player  $s$  under the matching state  $\Phi$ .

Note that the above definition implies that if two SBSs want to switch between two RBs, the RBs involved must approve the swap. Condition 1) implies that the utilities of

all the involved players should not be reduced after the swap operation. Condition 2) indicates that at least one of the players' utilities is increased after the swap operation. This avoids looping between equivalent matchings where the utilities of all involved agents are indifferent.

### B. Proposed Spectrum Allocation Algorithm

In this subsection, we first propose an initialization algorithm (IA) based on the GS algorithm to obtain the initial matching state [29]. After the initialization, we proceed with swap operations among SBSs to further improve the performance.

1) *Initialization Algorithm*: In the initialization algorithm, SBSs and RBs first initialize their own preference lists. The list of all the SBSs that are not matched with any RB is denoted by  $UNMATCH$ . In the matching process, each SBS proposes to its most preferred RB, then each RB accepts the most preferred SBS and rejects the others. This process continues until the set  $UNMATCH$  goes empty. The details of the initialization algorithm are as shown in **Algorithm 1**.

---

#### Algorithm 1 Initialization Algorithm (IA)

---

- 1: Construct the preference lists of the SBSs  $BLIST_b, b \in SBS$ ; and the preference lists of the RBs  $RBLIST_m, m \in RB$ ;
  - 2: Construct the set of the SBSs that are not matched  $UNMATCH$ ;
  - 3: **while**  $UNMATCH \neq \emptyset$  **and**  $\exists BLIST_b \neq \emptyset$  **do**
  - 4:   **for**  $\forall b \in UNMATCH$  **do**
  - 5:     SBS  $b$  proposes to its most preferred RB that has never rejected it before;
  - 6:   **end for**
  - 7:   **for**  $\forall m \in RB$  **do**
  - 8:     **if**  $\sum_{b \in SBS} \eta_{m,b} \leq q_{max}$  **then**
  - 9:       RB  $m$  keeps all the proposed SBSs;
  - 10:      Remove the matched SBSs from  $UNMATCH$ ;
  - 11:     **else**
  - 12:       RB  $m$  keeps the most preferred  $q_{max}$  SBSs, and rejects the others;
  - 13:      Remove the matched SBSs from  $UNMATCH$ ; and keep the rejected SBSs in  $UNMATCH$ .
  - 14:     **end if**
  - 15:     Remove  $m$  from the preference lists of SBSs that have sent proposals;
  - 16:   **end for**
  - 17: **end while**
- 

2) *Swap Operations Enabled Matching Algorithm*: After the initialization of the matching state based on the IA, swap operations among SBSs are enabled to further improve the performance of the resource allocation algorithm. The details of the proposed swap operations enabled matching algorithm (SOEMA-1) is shown in **Algorithm 2**. SOEMA-1 is composed of three steps. Step 1 initializes the matching state based on the algorithm IA. Step 2 focuses on the the swap operations between the SBSs. Each SBS keeps searching for all the other SBSs to check whether there exists a swap-blocking pair. The

swap-matching process continues until there exists no swap-blocking pair, and then the algorithm goes to step 3, i.e., the end of the algorithm. Note that to prevent SBS  $b$  looping in the swap operations with another SBS  $b'$ , we set the flag  $\mathcal{SR}_{b,b'}$  to record the time that SBS  $b$  and  $b'$  swap their allocated RBs. Each SBS  $b$  can at most swap with another SBS  $b'$  twice.

---

#### Algorithm 2 Swap Operations Enabled Matching Algorithm (SOEMA-1)

---

- 1: – **Step 1: Initialization**
  - 2: Matching by the Initialization Algorithm (IA);
  - 3: Obtain the initial matching state:  $\Phi_0$ ;
  - 4: Initialize the number of swapping requests that SBS  $b$  sends to  $b'$ , i.e.,  $\mathcal{SR}_{b,b'} = 0$ ;
  - 5: – **Step 2: Swap-matching process**:
  - 6: For each SBS  $b$ , it searches for another SBS  $b'$  to check whether it is a swap-blocking pair;
  - 7: **if**  $(b, b')$  forms a swap-blocking pair along with  $m = \Phi(b)$ , and  $m' = \Phi(b')$ , as well as  $\mathcal{SR}_{b,b'} + \mathcal{SR}_{b',b} < 2$  **then**
  - 8:   Update the current matching state to  $\Phi_b^{b'}$ ;
  - 9:    $\mathcal{SR}_{b,b'} = \mathcal{SR}_{b,b'} + 1$ ;
  - 10: **else**
  - 11:   Keep the current matching state;
  - 12: **end if**
  - 13: **Repeat Step 2** until there is no swap-blocking pair.
  - 14: – **Step 3: End of the algorithm**
- 

3) *Irrational Swap Matching Decisions*: We observe that the final matching of the proposed algorithm SOEMA-1 is significantly affected by the initial matching state. Since the SBSs can swap only between their current matchings, a better matching state that can achieve higher sum rate many not be formed directly based on the current matching state. For example, if the current matching state is  $\{\{m, b\}, \{m', b'\}, \{m'', b''\}\}$  and the optimal matching<sup>3</sup> is  $\{\{m, b'\}, \{m', b''\}, \{m'', b\}\}$ , the optimal matching can not be reached if  $(b, b')$  (or  $(b', b'')$ ) is not a swap-blocking pair under the current matching state. Motivated to solve this issue, we introduce the concept of ‘*experimentation*’ [30] to explore the space of matching states. Experimentation enables a player to destabilize a state involving a dominated allocation, at the cost of a temporary loss in utility. In this case, we propose a novel experimentation enabled matching algorithm (SOEMA-2), as shown in **Algorithm 3**. In SOEMA-2, the initialization step is the same as that in SOEMA-1. During the swap-matching process, if a pair of SBS  $(b, b')$  forms a swap-blocking pair, the swap operation between  $b$  and  $b'$  happens with probability 1. Otherwise, the swap operation between  $b$  and  $b'$  happens with the probability  $\epsilon$  through experimentation. Note that  $0 < \epsilon \ll 1$  is a small number that corresponds to the probability that a player makes an irrational decision.  $rand$  in **Algorithm 3** is a random number generator, and  $t_{max}$  is the maximum number of iterations.

<sup>3</sup>The optimal matching here is defined as the matching that can achieve the highest sum  $\alpha$  fairness-based data rate of SCUs.

---

**Algorithm 3** Swap Operations Enabled Matching Algorithm (SOEMA-2)
 

---

```

1: – Step 1: Initialization
2: Matching by the Initialization Algorithm (IA), and obtain
   the initial matching state:  $\Phi_0$ ;
3: – Step 2: Swap-matching with experimentation enabled:
4: while  $t \leq t_{max}$  do
5:   For each SBS  $b$ , it searches for another SBS  $b'$  to check
   whether it is a swap-blocking pair;
6:   if  $(b, b')$  forms a swap-blocking pair along with  $m =$ 
    $\Phi(b)$ , and  $m' = \Phi(b')$  then
7:     Update the current matching state to  $\Phi_b^{b'}$ ;
8:   else
9:     if  $rand < \epsilon$  then
10:      Update the current matching state to  $\Phi_b^{b'}$ ;
11:    else
12:      Keep the current matching state;
13:    end if
14:  end if
15:   $t = t + 1$ ;
16: end while
17: – Step 3: End of the algorithm

```

---

### C. Property Analysis

Given the proposed SOEMA-1 above, we present some important remarks on the properties in terms of stability, convergence, complexity and optimality.

1) *Stability*: As stated in [18], there is no longer a guarantee that a traditional “pairwise-stability” exists when players care about more than their own matching. If a stable matching does exist, it can be computationally difficult to obtain. The authors in [28] focused on the *two-sided exchange-stable matchings*, which is defined as follows:

**Definition 3.** A matching  $\Phi$  is two-sided exchange-stable if there does not exist a swap-blocking pair.

The *two-sided exchange stability* is a distinct notion of stability compared to the traditional notion of stability of [18], but one that is relevant to our situation where agents can compare notes with each other.

**Lemma 1.** The final matching  $\Phi^*$  of SOEMA-1 is a two-sided exchange-stable matching.

*Proof.* See Appendix B.  $\square$

2) *Convergence*: We now prove the convergence of SOEMA-1 while the convergence of SOEMA-2 is usually not considered as it is constrained by the maximum number of iterations  $t_{max}$ .

**Theorem 1.** SOEMA-1 converges to a two-sided exchange stable matching  $\Phi^*$  within limited number of iterations.

*Proof.* See Appendix C.  $\square$

3) *Complexity*: The complexity of SOEMA-1 is composed of two main parts, i.e., the IA and the swap-matching phases. For the IA, the complexity of setting up the preference lists

of SBSs and RBs is  $\mathcal{O}(BM^2)$ . For the swap-matching phase, the number of iterations cannot be given in a closed form. This is because it is uncertain that at which step the algorithm converges to a two-sided exchange stable matching. This is a common problem in most heuristic algorithms. We will analyze the number of total iterations for different numbers of SBSs and RBs in Fig. 2, and more detailed analysis can be found in Section VI. Here, we give an upper bound of the complexity as follows:

**Theorem 2.** The complexity of SOEMA-1 is upper bounded by  $\mathcal{O}(B^2)$ .

*Proof.* Since we restrict that each SBS  $b$  can at most swap its allocated RB with another SBS  $b'$  twice, the number of potential swap operations is upper bounded by  $2 \times \binom{B}{2}$ . Therefore, the complexity of SOEMA-1 is upper bounded by  $\mathcal{O}(B^2)$ .  $\square$

The complexity of SOEMA-2 is restricted by the maximum number of iterations  $t_{max}$ . For traditional exhaustive searching method, the complexity increases exponentially with  $B$  and  $M$ , which is much higher than SOEMA-1 and SOEMA-2.

4) *Optimality*: We show below whether SOEMA-1 and SOEMA-2 can achieve an optimal matching.

**Theorem 3.** All local maxima of SCUs’ sum  $\alpha$  fairness-based sum rate corresponds to a two-sided exchange stable matching.

*Proof.* Assume that the SCUs’ sum  $\alpha$  fairness-based data rate of matching  $\Phi$  is a local maximum value. If  $\Phi$  is not a stable matching, it indicates that there exists a swap-blocking pair that can further improve the sum  $\alpha$  fairness-based data rate of SCUs. However, this is inconsistent with the assumption that  $\Phi$  is local optimal, and hence we conclude that  $\Phi$  is two-sided exchange stable.  $\square$

However, not all two-sided exchange stable matchings obtained from SOEMA-1 are local maxima of SCUs’ total  $\alpha$  fairness-based data rate. The reason can be given in a simple example: SBS  $b$  does not approve a swap matching with  $b'$  along with their current matched RBs  $m$  and  $m'$ , due to the fact that its utility is not improved after the swap operation. However,  $m$  and  $m'$  can benefit a lot via this swap operation, which further improves the sum of SCUs’  $\alpha$  fairness-based data rates. Of course, we can *force* the swap operation to happen, but this will obtain a weaker stability, as stated in [14]. Similarly, although SOEMA-2 allows to explore the space of matching states, it still can not guarantee the optimality of the final matching.

## V. SEQUENTIAL CONVEX PROGRAMMING FOR POWER CONTROL

In this section, we then consider the power control for each SBS. More particularly, for any given RB allocation result  $\lambda$ , the original problem in (11) reduces to the power allocation problem for a SBS  $b$  as follows:

$$\max_{\mathbf{a}_b} U_\alpha(R_b^m(\mathbf{a}_b)), \quad (16a)$$

$$s.t. \quad (11c), (11g), (11h), \quad (16b)$$

where  $\mathbf{a}_b$  is the power allocation vector of SBS  $b$  for its serving SCUs.

Because of the existence of the co-channel interference, (16) is a non-convex problem with respect to  $\mathbf{a}_b$ . Therefore, obtaining the global optimum is rather difficult. In this section, we would like to adopt the sequential convex programming to solve the power allocation problem of each SBS.

Based on the proof in [23], the following inequality for  $\gamma_{b,k}^m$  holds:

$$\log_2(1 + \gamma_{b,k}^m) \geq b_k \log_2 \gamma_{b,k}^m + c_k, \quad (17)$$

where  $b_k$  and  $c_k$  are defined as

$$b_k = \frac{\bar{\gamma}_{b,k,k}^m}{1 + \bar{\gamma}_{b,k,k}^m}, \quad (18)$$

$$c_k = \log_2(1 + \bar{\gamma}_{b,k,k}^m) - \frac{\bar{\gamma}_{b,k,k}^m}{1 + \bar{\gamma}_{b,k,k}^m} \log_2 \bar{\gamma}_{b,k,k}^m, \quad (19)$$

respectively. The bound is tight for  $\gamma_{b,k}^m = \bar{\gamma}_{b,k,k}^m$ .

Consequently, the lower bound to the objective function in (16) is obtained as

$$U_\alpha(R_{b,k}^m) + U_\alpha(R_{b,j}^m) \geq U_\alpha(\bar{R}_{b,k}^m) + U_\alpha(\bar{R}_{b,j}^m), \quad (20)$$

where  $\bar{R}_{b,k}^m = b_k \log_2(\gamma_{b,k}^m) + c_k$ ,  $\bar{R}_{b,j}^m = b_j \log_2(\gamma_{b,j}^m) + c_j$ .

To transform  $\bar{R}_{b,k}^m$  to a concave function, we set  $a_{b,k} = 2^{x_{b,k}}$ ,  $a_{b,j} = 2^{x_{b,j}}$  and define  $\mathbf{x}_b = [x_{b,k}, x_{b,j}]$ . Accordingly, a new optimization problem can be obtained from (16) and (20) as follows:

$$\max_{\mathbf{x}_b} (U_\alpha(\bar{R}_{b,k}^m) + U_\alpha(\bar{R}_{b,j}^m)), \quad (21a)$$

$$s.t. \quad 2^{x_{b,k}} + 2^{x_{b,j}} \leq 1, \quad (21b)$$

**Proposition 1.** *The rewritten optimization problem in (21) is a convex optimization problem with respect to  $\mathbf{x}_b$ .*

*Proof.* See Appendix D.  $\square$

Since the problem in (21) is a convex optimization problem, we iteratively update the power allocation vector  $\mathbf{a}_b$  by solving (21) to tighten the lower bound in (20) until convergence. The details of the proposed power allocation algorithm is shown in **Algorithm 4**. The proposed algorithm consists of two main steps. The first step is the initialization step, where the initial power allocation vector  $\mathbf{a}_b(0)$  is set. The second step is the update step. In the  $i$ -th iteration of the second step, we set  $\bar{\gamma}_{b,k,k}^m = \gamma_{b,k}^m(i-1)$ , and subsequently derive the solution  $\mathbf{x}_b(i)$  by solving the convex optimization problem in (21). This process continues until the gap between the values of  $\gamma_{b,k}^m$  in the current iteration and that in the previous iteration is smaller than the threshold  $g_{thr}$ .

With the proposed subchannel allocation algorithms, i.e., IA, SOEMA-1, and SOEMA-2, and the power allocation algorithm, i.e., SCPAA, we then propose a joint spectrum allocation and power control algorithm (JSAPCA) to solve the SCUs' sum rate maximization problem in (11), as shown in **Algorithm 5**. In the first step of initialization, each SBS randomly allocates power to SCUs satisfying the constraints in (11g) and (11h). In the second step, the subchannel allocation

---

**Algorithm 4** Sequential Convex Programming Based Power Allocation Algorithm (SCPAA)

---

- 1: – **Initialization Phase:**
  - 2: Set  $i = 0$ .
  - 3: Initialize the power allocation vector  $\mathbf{x}_b(0)$ . Calculate  $\gamma_{b,k}^m(0)$  based on  $\mathbf{x}_b(0)$ .
  - 4: Set the convergence threshold  $g_{thr}$ .
  - 5: – **Update Phase:**
  - 6: **while**  $|\gamma_{b,k}^m(i) - \gamma_{b,k}^m(i-1)| \geq g_{thr}, \forall k$  **do**
  - 7:  $i = i + 1$ ;
  - 8: Set  $\bar{\gamma}_{b,k,k}^m = \gamma_{b,k}^m(i-1)$  and compute  $b_k$  and  $c_k$  according to (18) and (19);
  - 9: Solve the convex optimization problem in (21) and set the result as  $\mathbf{x}_b(i)$ ;
  - 10: Update  $\mathbf{a}_b(i)$ , where  $a_{b,k}(i) = 2^{x_{b,k}(i)}, \forall k$ ;
  - 11: Calculate  $\gamma_{b,k}^m(i), \forall k$  based on  $\mathbf{a}_b(i)$ ;
  - 12: **end while**
  - 13: **Result:**  $\mathbf{a}_b^* = \mathbf{a}_b(i)$ .
- 

---

**Algorithm 5** Joint Spectrum Allocation and Power Control Algorithm (JSAPCA)

---

- 1: – **Step 1: Initialization:**
  - 2: Randomly allocate power for SCUs served by each SBS, where  $\mathbf{a}$  should satisfy the constraints in (11g) and (11h).
  - 3: Set  $i = 0$ ;
  - 4: – **Step 2: Joint Spectrum Allocation and Power Control**
  - 5: **repeat**
  - 6: Update the subchannel allocation result  $\lambda$  according to IA, SOEMA-1 or SOEMA-2;
  - 7: Given  $\lambda$ , update the power allocation vector  $\mathbf{a}$  according to SCPAA.
  - 8:  $i = i + 1$ ;
  - 9: **until** convergence **or**  $i \geq i_{max}$ .
  - 10: Resource allocation result:  $\lambda, \mathbf{a}$ .
- 

is first performed based on the current value of  $\mathbf{a}$ . Subsequently, the power allocation algorithm is executed based on the subchannel allocation result. This process is repeated for a maximum number of  $i_{max}$  iterations, where the joint solution is obtained.

**Theorem 4.** *The proposed algorithm JSAPCA with SOEMA-1 is guaranteed to converge.*

*Proof.* Each iteration of the joint algorithm JSAPCA consists of two main stages: spectrum allocation and power control. We have proved in Theorem 1 that the sum  $\alpha$ -fairness based data rate of SCUs is improved after the swap operations in SOEMA-1. For the power allocation algorithm SCPAA, the sum  $\alpha$  utility is guaranteed to not decrease according to the inequality in (20). We assume that  $U_{\alpha-total} R_{b,k}^m(i)$  and  $U_{\alpha-total} R_{b,k}^m(i')$  are the sum utilities of SCUs at the beginning and end of the  $i$ -th iteration. We have the following inequality

$$U_{\alpha-total} R_{b,k}^m(i') > U_{\alpha-total} R_{b,k}^m(i). \quad (22)$$

Since the upper bound of the sum rate of SCUs exists due to the limited resources, we can conclude that the joint algorithm



JSAPCA with SOEMA-1 converges within limited number of iterations.  $\square$

For JSAPCA with IA and SOEMA-2, the maximum number of iterations is constrained by the value of  $i_{max}$ , as shown in **Algorithm 5**.

## VI. NUMERICAL RESULTS

In this section, we investigate the performance of the proposed resource allocation algorithm through simulations. The adopted simulation parameters are given in Table II. For convenience, we refer to the JSAPCA with IA as JSAPCA-1, the JSAPCA with SOEMA-1 as JSAPCA-2, and the JSAPCA with SOEMA-2 as JSAPCA-3. The optimal performance which is obtained by the exhaustive searching method for both spectrum allocation and power control is given as the baseline. We compare JSAPCA-1, JSAPCA-2, and JSAPCA-3 in the NOMA-HetNets system to show differences among their performances. In addition, we also consider the performance of the traditional OMA-HetNets system where each SBS communicates with at most one SCU in a transmission interval. In order to have a fair comparison, the resource allocation result for the OMA-based HetNets is also obtained by utilizing JSAPCA-1, JSAPCA-2 and JSAPCA-3, respectively. The settings of the proposed algorithms and benchmarks are summarized in Table III.

TABLE II: Parameter Values Used in Simulations

Macro cell radius	300 m
Small cell radius	30 m
Transmit power of MBS	43 dBm
Transmit power of SBSs	23 dBm
Noise power spectral density	-174 dBm/Hz
Path-loss exponent	4
Interference threshold at each MCU	-70 dBm

TABLE III: Algorithm Settings

Algorithm	Subchannel Allocation	Power Control	Multiple Access
Optimal Solution	Exhaustive search	Exhaustive search	NOMA
JSAPCA-1	IA	SCPAA	NOMA
JSAPCA-2	SOEMA-1	SCPAA	NOMA
JSAPCA-3	SOEMA-2	SCPAA	NOMA
JSAPCA-1 (OMA)	IA	SCPAA	OMA
JSAPCA-2 (OMA)	SOEMA-1	SCPAA	OMA
JSAPCA-3 (OMA)	SOEMA-2	SCPAA	OMA

Fig. 2 illustrates the convergence of the proposed algorithms, i.e., IA, SOEMA-1 and SOEMA-2, with different numbers of RBs  $M$  and SBSs  $B$ . It can be seen that IA and SOEMA both converge within a small number of iterations for different values of  $M$  and  $B$ . Besides, both IA and SOEMA need more iterations to converge with a larger number of RBs and SBSs. For example, when  $B = 7, M = 5$ , SOEMA and IA converge in less than 6 iterations on average. When  $B = 10, M = 5$ , SOEMA and IA converge to a stationary point

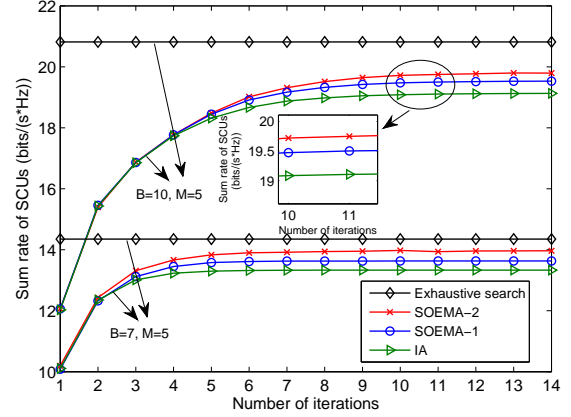


Fig. 2: Convergence of the proposed matching algorithms with different numbers of RBs and SBSs.

at around 12 iterations. This is due to the fact that additional players participating in the matching game results in additional searching dimensions in the possible matching solutions. It is also shown in Fig. 2 that the proposed algorithm performs very close to the exhaustive searching based spectrum allocation. In particular, for the case of  $B = 10, M = 5$ , SOEMA-2 gets around 93% of the sum rate of SCUs achieved by the exhaustive searching method.

Fig. 3 depicts the SCUs' sum rate with number of iterations in JSAPCA-2, under the case of  $M = 5$ . In particular, JSAPCA-2 needs more iterations to converge when the number of SBSs  $B$  gets larger. For example, when  $B = 8$ , the number of iterations for convergence is 20 on average. In the case of  $B = 11$ , JSAPCA-2 converges to a stationary point after 4 iterations on average. This is due to the fact that more SBSs need to be coordinated, which causes the higher dependency between spectrum allocation and power control. We can also observe that, in the case of  $B = 11$ , JSAPCA-2 gets roughly 91% of the SCUs' sum rate achieve by the optimal solution.

Fig. 4 plots the sum rate of SCUs versus different numbers of SBSs in the network, for  $M = 7$  and  $q_{max} = 2$ . As can be observed, the sum rate increases monotonically with the number of SBSs due to the exploitation of multi-user diversity gain. Fig. 4 also shows that JSAPCA-2 achieves a higher sum rate compared to JSAPCA-1 due to the involvement of the swap operations between the potential swap-blocking pairs. Besides, JSAPCA-3 further improves the performance of JSAPCA-2 because of the 'experimentation' action to explore the space of matching states. Compared to the traditional OMA system, the NOMA-enhanced HetNets can achieve higher sum rate since it exploits not only the frequency domain but also the power domain for multiple access. In particularly, at the point of  $B = 18, M = 7$ , JSAPCA-2 achieves roughly a 10%, 49% and 55% higher sum rate than JSAPCA-1, JSAPCA-2 (OMA), and JSAPCA-1 (OMA), respectively.

In Fig. 5, we investigate the number of scheduled SBSs versus the number of SBSs with  $M = 10$  in the NOMA system in HetNets. Here, the number of scheduled SBSs is defined as the average number of simultaneously scheduled SBSs in a

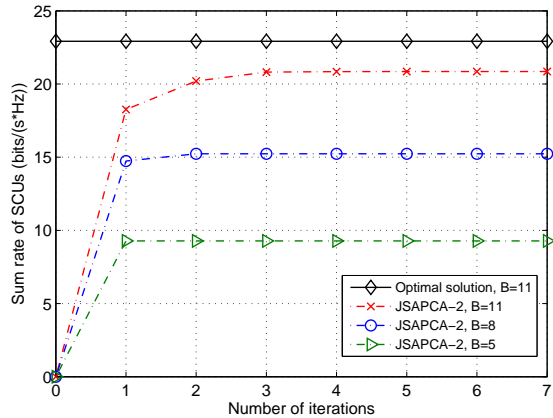


Fig. 3: Convergence of JSAPCA-2 with different numbers of SBSs, with  $M = 5$ .

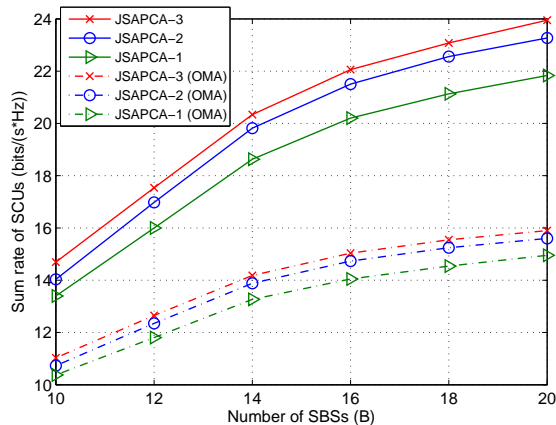


Fig. 4: Sum rate of the SCUs with different numbers of small cells, with  $M = 7$ .

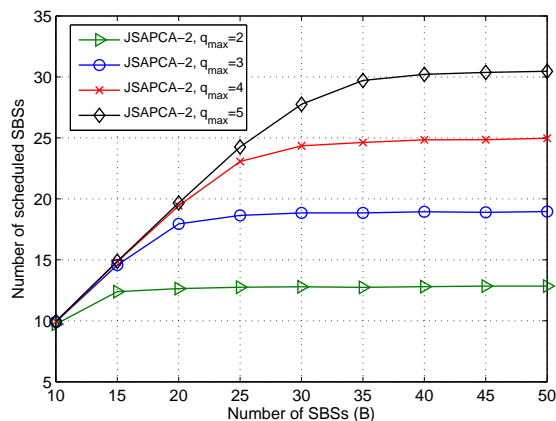


Fig. 5: Number of scheduled SBSs with different numbers of SBSs in the network, with  $M = 10$ .

transmission interval. We observe that the number of scheduled SBSs increase monotonically with the total number of SBSs. However, the increasing trend becomes slower as the total

number of SBSs becomes larger. This is due to the fact that the SBSs causing server co-channel interference to others may not be allocated any RB for the maximization of SCUs' sum rate as well as the satisfaction of interference constraints of MCUs. Besides, the proposed algorithm is capable of accommodating more SBSs when the maximum number of allowed SBSs on each RB gets larger, since more SBSs have the opportunity to get access to the RBs.

Fig. 6 demonstrates the sum rate of SCUs versus different maximum numbers of SBSs allowed on each RB with the RBs' number of  $M = 5$ . One can observe that with a fixed value of SBSs' number  $B$ , the sum rate of SCUs grows to a fixed value as the quota  $q_{max}$  increases since all the SBSs have been matched after  $q_{max}$  reaches  $B/M$ . In particular, for the case of  $B = 20$ , the SCUs' sum rate reaches a stable value when  $q_{max} > 4$ . For the case of  $B = 40$ , the sum rate keeps increasing because  $B/M > 7$ . However, the growth rate gets smaller with larger value of  $q_{max}$  due to the enhanced interference on each RB.

Fig. 7 shows the resource allocation fairness versus the total number of SBSs in the network, for a fixed RB's number  $M = 10$ . To evaluate the fairness of the proposed algorithm, we adopt the Jain's fairness index [31] which can be calculated as  $\frac{(\sum_{b=1}^B (R_{b,k}^m + R_{b,j}^m))^2}{2 \times B \sum_{b=1}^B (R_{b,k}^m{}^2 + R_{b,j}^m{}^2)}$ . The value of Jain's fairness index is between the range of 0 and 1. The fairest resource allocation is obtained when the value equals to 1, which indicates that all users enjoy the same data rate. One can observe that the fairness index of the proposed algorithm decreases with the number of SBSs in the network. This is due to the fact that higher number of SBSs contributes to more severe competition on limited spectrum resources, and hence more SBSs with poor channel conditions may not be accessed to the network. This phenomenon is consistent with Fig. 5 showing that the number of scheduled SBSs increases non-linearly with the total number of SBSs in the network. Besides, it is also worth noting that the proposed algorithm can achieve a higher fairness index when the maximum number of SBSs allowed on each RB, i.e.,  $q_{max}$ , gets larger. Actually, as  $q_{max}$  increases, the proposed algorithm is capable of multiplexing more SBSs on each RB, which increases the utilization of multiuser diversity.

## VII. CONCLUSIONS

In this paper, the spectrum allocation and power control problems in NOMA-enhanced HetNets were jointly studied, with the aim of maximizing the sum rate of SCUs while considering the fairness issues. By formulating the spectrum allocation problem as a many-to-one matching game with peer effects, a low-complexity algorithm based on the swap operations was proposed to enable SBSs and RBs to effectively interact with each other. In addition, the 'experimentation' action was utilized to further improve the performance by exploring the space of matching states. It was proved mathematically that the matching algorithm converged to a two-sided stable state within limited number of iterations. For solving the power allocation problem, the sequential convex programming was adopted to approximate the non-convex

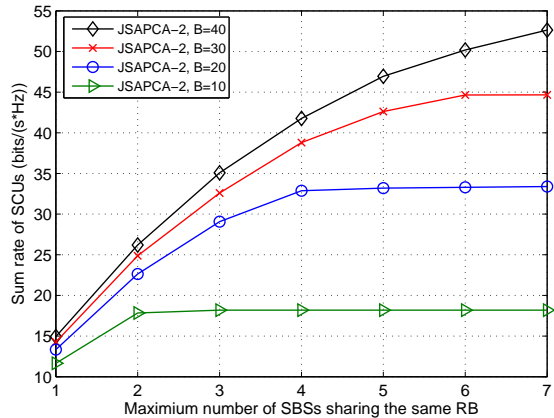


Fig. 6: Sum rate of SCUs with different maximum numbers of SBSs allowed on each RB, with  $M = 5$ .

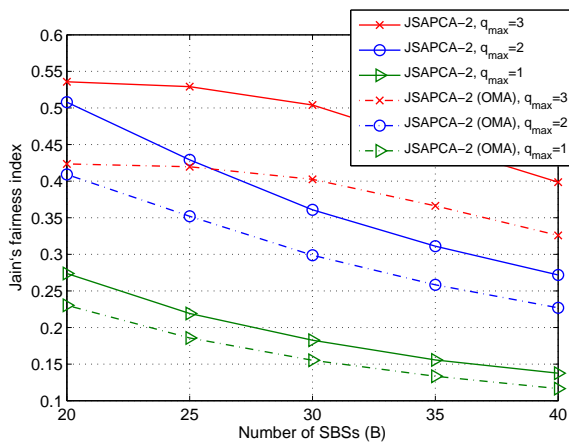


Fig. 7: SCUs fairness index with different numbers of SBSs in the network, with  $M = 10$ .

problem to a convex one and update the power allocation result iteratively. Numerical results demonstrated that NOMA-enhanced HetNets had more potential benefits than traditional OMA-based HetNets in achieving higher sum rate and massive connectivity.

#### APPENDIX A

*Proof of Remark 2:* Faced with a set  $\mathcal{S}$  of SBSs, RB  $m$  can determine which subset of  $\mathcal{S}$  it would most prefer to match with. We call this RB  $m$ 's choices from  $\mathcal{S}$ , and denote it by  $\text{Ch}_m(\mathcal{S}) = \mathcal{S}'$ . That is, for any subset  $\mathcal{S}$  of SBS, the most preferred set of RB  $m$  is  $\mathcal{S}'$  satisfying:  $\forall \mathcal{S}'' \subset \mathcal{S}, \mathcal{S}'' \neq \mathcal{S}' \Rightarrow \mathcal{S}' \succ_m \mathcal{S}''$ . A RB  $m$ 's preferences over sets of SBSs has the property of *substitutability* if, for any set  $\mathcal{S}$  that contains SBSs  $b$  and  $b'$ , if  $b$  is in  $\text{Ch}_m(\mathcal{S})$ , then  $b$  is in  $\text{Ch}_m(\mathcal{S} \setminus \{b'\})$ .

However, in the formulated game model, due to the existence of co-tier interference, the achievable rate of RB  $m$  with SBS  $b$  may change after  $b'$  is unmatched with  $m$ , and therefore,  $b$  may not be in the preferred set any more, which is concluded that the formulated game model does not have the property of *substitutability*.

#### APPENDIX B

*Proof of Lemma 1:* Assume that there exists a swap-blocking pair  $(b, b')$  in the final matching  $\Phi^*$  satisfying that  $\forall s \in \{b, b', \Phi(b), \Phi(b')\}, U_s((\Phi^*)_{b'}^{b'}) \geq U_s(\Phi^*)$  and  $\exists s \in \{b, b', \Phi(b), \Phi(b')\}$ , such that  $U_s((\Phi^*)_{b'}^{b'}) > U_s(\Phi^*)$ . According to SOEMA-1, the algorithm does not terminate until all the swap-blocking pairs are eliminated. In other words,  $\Phi^*$  is not the final matching, which causes conflict. Therefore, there does not exist a swap-blocking pair in the final matching, and thus we can conclude that the proposed algorithm reaches a two-sided exchange stability in the end of the algorithm.

#### APPENDIX C

*Proof of Theorem 1 :* The convergence of SOEMA-1 depends mainly on Step 2 in **Algorithm 2**. According to Definition 2, after each swap operation between SBS  $b$  and  $b'$  along with their corresponding matched RBs  $m, m'$ , the utilities of  $m$  and  $m'$  satisfy:  $U_m(\Phi_b^{b'}) \geq U_m(\Phi)$ ,  $U_{m'}(\Phi_{b'}^{b'}) \geq U_{m'}(\Phi)$ , in which at least one of the equalities does not stand. Since the utility of each RB is defined as the sum  $\alpha$  fairness-based data rate of its occupying SCUs as in (14), the following inequality holds:

$$U_{\alpha\text{-total}} R_{b,k}^m(\Phi_b^{b'}) > U_{\alpha\text{-total}} R_{b,k}^m(\Phi), \quad (23)$$

where  $U_{\alpha\text{-total}} R_{b,k}^m = \sum_{b=1}^B \sum_{m=1}^M U_{\alpha}(R_b^m)$ , which is the sum  $\alpha$  fairness-based data rate of all the SCUs in the network. Note that the number of iterations of SOEMA-1 is limited since the number of players is limited and the system sum rate has an upper bound due to the limited spectrum resources. Therefore, there exists a swap operation after which no swap-blocking pair can further improve the sum rate of SCUs. SOEMA-1 then converges to the final matching  $\Phi^*$  which is stable as proved in **Lemma 1**.

#### APPENDIX D

*Proof of Proposition 1:* We can rearrange  $\bar{R}_{b,k}^m$  as the following:

$$\begin{aligned} \bar{R}_{b,k}^m = & b_k [x_{b,k} - \log_2(|f_{b,k}^m|^2 p_b 2^{x_{b,j}} + I_{co}^k + I_{cr}^k + \sigma^2)] \\ & + b_k \log_2(|f_{b,k}^m|^2 p_b) + c_k. \end{aligned} \quad (24)$$

$\bar{R}_{b,k}^m$  is a concave function of  $\mathbf{x}_b$  because of the convexity of the log-sum-exp function [32]. Furthermore, as the  $\alpha$ -fair utility function is strictly increasing and concave for any given  $\alpha$ , their composition,  $U_{\alpha}(\bar{R}_{b,k}^m)$  is also a concave function of  $\mathbf{x}_b$  [32]. Since the objective function in (21a) is a summation of the concave terms of  $\mathbf{x}_b$ , it is straightforward to conclude that (21a) is also a concave function of  $\mathbf{x}_b$ . Therefore, the optimization problem in (21) is a standard convex optimization problem with respect to  $\mathbf{x}_b$ .

## REFERENCES

- [1] H. S. Dhillon, R. K. Ganti, F. Baccelli, and J. G. Andrews, "Modeling and analysis of k-tier downlink heterogeneous cellular networks," *IEEE J. Sel. Areas Commun.*, vol. 30, no. 3, pp. 550–560, Apr. 2012.
- [2] X. Lagrange, "Multitier cell design," *IEEE Commun. Mag.*, vol. 35, no. 8, pp. 60–64, Aug. 1997.
- [3] Q. Ye, B. Rong, Y. Chen, M. Al-Shalash, C. Caramanis, and J. G. Andrews, "User association for load balancing in heterogeneous cellular networks," *IEEE Trans. Wireless Commun.*, vol. 12, no. 6, pp. 2706–2716, Jun. 2013.
- [4] D. Fouladivanda and C. Rosenberg, "Joint resource allocation and user association for heterogeneous wireless cellular networks," *IEEE Trans. Wireless Commun.*, vol. 12, no. 1, pp. 248–257, Jan. 2013.
- [5] S. Bayat, R. H. Louie, Z. Han, B. Vucetic, and Y. Li, "Distributed user association and femtocell allocation in heterogeneous wireless networks," *IEEE Trans. Commun.*, vol. 62, no. 8, pp. 3027–3043, Jul. 2014.
- [6] M. Hasan and E. Hossain, "Distributed resource allocation in D2D-enabled multi-tier cellular networks: An auction approach," in *Proc. of the IEEE Int. Conf. on Commun. (ICC)*, London, Jun. 2015, pp. 2949–2954.
- [7] Z. Ding, Y. Liu, J. Choi, Q. Sun, M. Elkashlan, C.-L. I, and H. V. Poor, "Application of non-orthogonal multiple access in LTE and 5G networks," *IEEE Commun. Mag.*, to appear in 2016.
- [8] Z. Ding, Z. Yang, P. Fan, and H. V. Poor, "On the performance of non-orthogonal multiple access in 5G systems with randomly deployed users," *IEEE Signal Process. Lett.*, vol. 21, no. 12, pp. 1501–1505, Dec. 2014.
- [9] S. Timotheou and I. Krikidis, "Fairness for non-orthogonal multiple access in 5G systems," *IEEE Signal Process. Lett.*, vol. 22, no. 10, pp. 1647–1651, Oct. 2015.
- [10] S. Shi, L. Yang, and H. Zhu, "Outage balancing in downlink nonorthogonal multiple access with statistical channel state information," *IEEE Trans. Wireless Commun.*, vol. 15, no. 7, pp. 4718–4731, Jul. 2016.
- [11] J. Cui, Z. Ding, and P. Fan, "A novel power allocation scheme under outage constraints in noma systems," *IEEE Signal Process. Lett.*, vol. 23, no. 9, pp. 1226–1230, Aug. 2016.
- [12] Y. Liu, Z. Ding, M. Elkashlan, and H. V. Poor, "Cooperative non-orthogonal multiple access with simultaneous wireless information and power transfer," *IEEE J. Sel. Areas Commun.*, vol. 34, no. 4, pp. 938–953, Apr. 2016.
- [13] Y. Sun, D. W. K. Ng, Z. Ding, and R. Schober, "Optimal joint power and subcarrier allocation for full-duplex multicarrier non-orthogonal multiple access systems," *submitted to IEEE Trans. Wireless Commun.*, 2016. [Online]. Available: <https://arxiv.org/abs/1607.02668>
- [14] B. Di, L. Song, and Y. Li, "Sub-channel assignment, power allocation, and user scheduling for non-orthogonal multiple access networks," *IEEE Trans. Wireless Commun.*, vol. 15, no. 11, pp. 7686–7698, Nov. 2016.
- [15] F. Fang, H. Zhang, J. Cheng, and V. C. M. Leung, "Energy-efficient resource allocation for downlink non-orthogonal multiple access network," *IEEE Trans. Commun.*, vol. 64, no. 9, pp. 3722–3732, Sep. 2016.
- [16] Z. Wei, D. W. K. Ng, and J. Yuan, "Power-efficient resource allocation for MC-NOMA with statistical channel state information," *arXiv preprint arXiv:1607.01116*, 2016.
- [17] Y. Liu, M. Elkashlan, Z. Ding, and G. K. Karagiannidis, "Fairness of user clustering in MIMO non-orthogonal multiple access systems," *IEEE Commun. Lett.*, vol. 20, no. 7, pp. 1465–1468, Jul. 2016.
- [18] A. E. Roth and M. A. O. Sotomayor, *Two-sided matching: A study in game-theoretic modeling and analysis*. Cambridge University Press, 1992, no. 18.
- [19] Y. Gu, W. Saad, M. Bennis, M. Debbah, and Z. Han, "Matching theory for future wireless networks: fundamentals and applications," *IEEE Commun. Mag.*, vol. 53, no. 5, pp. 52–59, May 2015.
- [20] D. F. Manlove, *Algorithmics of matching under preferences*. World Scientific, 2013, vol. 2.
- [21] L. Lei, D. Yuan, C. K. Ho, and S. Sun, "Joint optimization of power and channel allocation with non-orthogonal multiple access for 5G cellular systems," in *Proc. of the IEEE Global Commun. Conf. (GLOBECOM)*, San Diego, Dec. 2015, pp. 1–6.
- [22] J. Mo and J. Walrand, "Fair end-to-end window-based congestion control," *IEEE/ACM Trans. on Networking*, vol. 8, no. 5, pp. 556–567, Oct. 2000.
- [23] J. Papandriopoulos and J. S. Evans, "Low-complexity distributed algorithms for spectrum balancing in multi-user DSL networks," in *Proc. of the IEEE Int. Conf. on Commun. (ICC)*, vol. 7, Istanbul, Jun. 2006, pp. 3270–3275.
- [24] Y. Gu, Y. Zhang, M. Pan, and Z. Han, "Matching and cheating in device to device communications underlying cellular networks," *IEEE J. Sel. Areas Commun.*, vol. 33, no. 10, pp. 2156–2166, Oct. 2015.
- [25] M. Hasan and E. Hossain, "Distributed resource allocation for relay-aided device-to-device communication: A message passing approach," *IEEE Wireless Commun.*, vol. 13, no. 11, pp. 6326–6341, Jul. 2014.
- [26] B. Dutta and J. Massó, "Stability of matchings when individuals have preferences over colleagues," *Journal of Economic Theory*, vol. 75, no. 2, pp. 464–475, Jan. 1997.
- [27] I. E. Hafalir, "Stability of marriage with externalities," *International Journal of Game Theory*, vol. 37, no. 3, pp. 353–369, Mar. 2008.
- [28] E. Bodine-Baron, C. Lee, A. Chong, B. Hassibi, and A. Wierman, "Peer effects and stability in matching markets," in *Algorithmic Game Theory*. Springer, Apr. 2011, pp. 117–129.
- [29] Y. Zhang, Y. Gu, M. Pan, and Z. Han, "Distributed matching based spectrum allocation in cognitive radio networks," in *Proc. of the IEEE Global Commun. Conf. (GLOBECOM)*, Austin, Dec. 2014, pp. 864–869.
- [30] T. Arnold and U. Schwalbe, "Dynamic coalition formation and the core," *Journal of Economic Behavior & Organization*, vol. 49, no. 3, pp. 363–380, Nov. 2002.
- [31] R. Jain, D.-M. Chiu, and W. R. Hawe, *A quantitative measure of fairness and discrimination for resource allocation in shared computer system*. Eastern Research Laboratory, Digital Equipment Corporation Hudson, MA, USA, Sep. 1984, vol. 38.
- [32] S. Boyd and L. Vandenberghe, *Convex optimization*. Cambridge university press, 2004.